

Andy Gradel^{1,*}
Joachim Alfred Wüning²
Tobias Plessing¹
Andreas Jess³


Adsorption of Naphthalene on Activated Wood Charcoal Derived from Biomass Gasification

During gasification and/or pyrolysis of wooden biomass, charcoal is formed as a solid intermediate or product. In CO₂- and H₂O-rich atmospheres at high temperatures, a high specific surface area of several 100 m² per gram of charcoal may be reached. Common biomass gasifiers aim at a charcoal conversion of 100 %. Up to now, the option of a subsequent usage of the charcoal for adsorption of tar compounds has rarely been considered but is an interesting option to produce a clean syngas in a downstream adsorption unit. Experimental studies show an adsorption capacity of up to 0.4 g of tar per gram of charcoal using naphthalene as a model substance for tar. Respective adsorption isotherms, breakthrough curves in a fixed-bed adsorber, and a kinetic breakthrough model are presented.

Keywords: Activated wood charcoal, Adsorption, Biomass gasification, Breakthrough modeling, Naphthalene

Received: November 27, 2020; *revised:* February 18, 2021; *accepted:* February 25, 2021

DOI: 10.1002/ceat.201900632

 This is an open access article under the terms of the Creative Commons Attribution License, which permits use, distribution and reproduction in any medium, provided the original work is properly cited.

1 Introduction

Thermal gasification of biomass is an attractive technology for the sustainable conversion to syngas (fuel gas). Unfortunately, the raw gas frequently contains high amounts of mostly aromatic hydrocarbons, formed during the pyrolysis of the biogenic feedstock. These compounds have to be separated from the crude syngas before its use, e.g., in a chemical synthesis such as Fischer-Tropsch or methanol synthesis or as fuel gas in an electricity and/or cogeneration unit. These unwanted higher hydrocarbon species are commonly summarized as tars.

The adsorption experiments and modeling results presented in this work were part of a research and development (R&D) project for a new approach to biomass gasification. This process aims at the production of a clean syngas by using a concurrent moving-bed gasification reactor combined with a gas cleanup in a subsequent cooled adsorption section. The charcoal produced in the gasifier is thereby directly used as adsorbent for the tar species. Hence, the conversion of the charcoal primarily formed by pyrolysis by subsequent gasification with steam and carbon dioxide (to CO and H₂) has to be adjusted within the gasifier to ensure a yield of coke sufficient for adsorption. On the other hand, a certain degree of conversion of the pyrolysis coke with CO₂ and/or steam is needed to reach a high internal surface area of the adsorbent. The overall process and further information of this specific gasification process are given in a previous publication [1] and a respective patent [2].

Activated carbon is the most common material for adsorption applications that offers a large adsorption capacity for various compounds. The high capacity results from large internal surfaces and well adjustable pore structures [3]. As the reduc-

tion of fossil raw materials for the production of activated carbon is currently an environmental goal, a lot of work is done on the use of biogenic feedstock materials. Danish and Ahmad [4] give a present overview of the production and application of activated carbon from wooden raw materials, and they refer to several studies, where activated wood-derived charcoals are applied for water and gas cleaning.

Gaseous naphthalene, which is selected in this work as a model substance for the tar species, has also been examined as adsorbate on commercial and recycled activated carbon by Liu et al. [5] and Mastral et al. [6]. Nevertheless, these experiments were performed at higher temperatures and with carbon derived from lignite or biomasses such as coconut shells. Therefore, these results are not applicable to the conditions and the feedstock material (wood pellets) used here. Shen et al. [7] took different activated char samples from biomass pyrolysis to adsorb phenol as a model substance for tar compounds. A maximum adsorption capacity of more than 0.7 g g⁻¹ could

¹Dr.-Ing. Andy Gradel, Prof. Dr.-Ing. Tobias Plessing
andy.gradel@hof-university.de

Institute for Water- and Energy Management, University of Applied Sciences Hof, Alfons Goppel Platz 1, 95028 Hof, Germany.

²Dr. Joachim Alfred Wüning

WS Wärmeprozessstechnik GmbH, Dornierstrasse 14, 71272 Rellingen, Germany.

³Prof. Dr.-Ing. Andreas Jess

Chair of Chemical Engineering, Center of Energy Technology (ZET), University of Bayreuth, Universitätsstrasse 30, 95447 Bayreuth, Germany.

be proved in this study but also without an investigation of the influence of temperature. In the work of Zhang et al. [8], the adsorption of benzene and naphthalene on two different activated carbons was examined for various temperatures. The results can also not be applied to this work since the relation of char conversion and adsorption capacity was not taken into account.

For an optimum design of the overall gasification process with integrated adsorption for gas cleanup, the adsorption capacity and kinetics were examined in this work as a function of the tar concentration and temperature of adsorption. In addition, the internal surface of the charcoal used for adsorption was also varied by pyrolysis of wood pellets and subsequent gasification (to a certain degree) with CO₂. Finally, adsorption experiments in a fixed bed were conducted, and the resulting breakthrough curves were modeled.

2 Experimental Setup and Sample Preparation

For the determination of adsorption isotherms and breakthrough curves, a lab-scale adsorption unit with a fixed-bed reactor was employed (Fig. 1; conditions see Tab. 1). The temperature of the bed was controlled by an oil thermostat. The naphthalene concentration in the inlet gas stream was adjusted by a saturator with nitrogen as carrier gas. The temperature of the saturator was also controlled by an oil thermostat. An additional nitrogen flow was added just behind the saturator. The nitrogen flows were controlled by mass flow controllers. The concentration of naphthalene was in a range of only 75 mg m⁻³ (NTP) up to 8 g m⁻³ (NTP).

For the online detection of the naphthalene concentration at the outlet of the adsorber and the breakthrough of the tar (here naphthalene), respectively, air was added downstream of the adsorber for naphthalene combustion in a subsequent combustion tube. This enabled the (indirect) online detection of naphthalene (as CO₂) with a respective CO₂ gas analyzer and prevented the deposition of naphthalene in the exhaust gas line. The combustion tube was heated electrically to 900 °C and filled with steel wool to maximize the surface and to catalyze the combustion step. All experiments were conducted with an

Table 1. Reactor dimensions, settings, and sample properties for the adsorption experiments.

Parameter	Value
Inner reactor diameter [mm]	25
Length of adsorption bed (5 g charcoal) [mm]	30–70
Porosity of fixed bed [–]	0.4
Adsorption temperature range [°C]	70–120
Total pressure [bar]	1 (atmospheric)
Concentration of naphthalene [g m ⁻³ (NTP)]	0.075–8
Mass of charcoal [g]	5 ± 0.1
Conversion of raw charcoal (derived by wood pyrolysis) [–]	0.0, 0.23, 0.33, 0.59
Particle diameter [mm]	4
Particle length (average) [mm]	10
Particle porosity [–]	0.55, 0.66, 0.7, 0.82
Particle density [kg m ⁻³]	824, 630, 550, 341
Overall gas flow [L h ⁻¹]	200

overall volumetric flow rate of 200 L h⁻¹ (NTP) and at atmospheric pressure. The determination of the equilibrium adsorption load was conducted by integrating the breakthrough curves and validated by a gravimetric analysis of the sample after the inlet concentration of naphthalene was reached at the outlet of the adsorber.

In the gasification process briefly described above, the charcoal is derived from the partial gasification of raw charcoal formed by wood pyrolysis. The properties of the charcoal, above all the internal surface area, strongly depend on the degree of conversion by gasification. For the determination of the influence of the conversion on the internal surface area of the residual carbon, different charcoal samples were produced. Standardized wood pellets from southern Germany in accordance with the local standard [9] were chosen; for characteristic data of this raw material see [1].

Raw charcoal samples were produced by heating up the wood pellets (1.5 kg) stepwise in a nitrogen flow in batch experiments until a temperature of 900 °C was reached (details in [10]). Thereafter, the char was partly gasified by CO₂ (35 % in nitrogen) at 800 °C. The conversion of the charcoal (throughout this paper indicated with symbol *X*) was monitored by a gas analyzer for CO and CO₂ and respective integration of the measured signals. Samples were taken at conversion degrees *X* of 0, 0.23, 0.33, and 0.59 with respect to the initial charcoal mass after pyrolysis. The conversion was limited to 60 %, as the mechanical stability of the charcoal then gets too low. Subsequently, the charcoals were used for adsorption experiments with the conditions mentioned in Tab. 1.

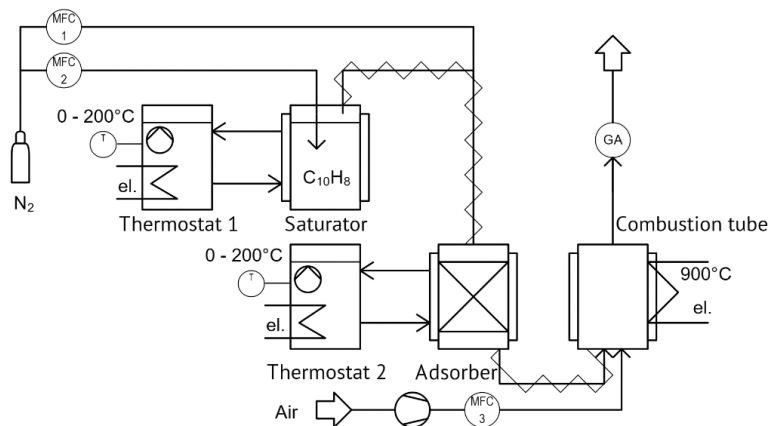


Figure 1. Experimental setup for the analysis of adsorption properties.

3 Model Equations

A transient one-dimensional adsorption model has been developed for the prediction of breakthrough curves. The respective mass balance considers the distribution of naphthalene in the gas phase and the adsorption on the charcoal.

$$\frac{\partial \gamma_n}{\partial t} = -\frac{u_s}{\varepsilon_b} \frac{\partial \gamma_n}{\partial z} - \frac{\rho_b k_{LDF}}{\varepsilon_b} (L_{eq} - L_{ads}) \quad (1)$$

$$\frac{\partial L_{ads}}{\partial t} = k_{LDF} (L_{eq} - L_{ads}) \quad (2)$$

γ_n ¹⁾ denotes the naphthalene concentration in the gas phase (kg m^{-3}) under the conditions of adsorption, i.e., T_{ad} and p_{ad} , u_s is the superficial gas velocity (at T_{ad} and p_{ad}), ρ_b is the bulk density of the charcoal (kg m^{-3}), ε_b is the bulk porosity, and L_{eq} and L_{ads} are the maximum (equilibrium) and the current (mean) adsorption loads of the charcoal particles (in kg naphthalene per kg charcoal), respectively. The linear driving force approach was used here with k_{LDF} (Eq. (3)) as the overall mass transfer coefficient for a spherical particle; the derivation of k_{LDF} is given in [11].

$$k_{LDF} = \frac{60 D_{app}}{d_p^2} \quad (3)$$

For the approximation of the diffusion into the cylindrical char particles, the diameter of a sphere with an equivalent volume-to-surface ratio is used (here 5 mm). The apparent diffusion coefficient D_{app} in Eq. (3) is given by:

$$D_{app} = \frac{D_{eff}}{\varepsilon_p + K_p} \quad (4)$$

ρ_p is the porosity of the charcoal particles, and the factor K_p is a function of the gradient of the adsorption isotherm:

$$K_p = \rho_p \frac{\partial L_{eq}}{\partial \gamma_n} \quad (5)$$

D_{app} (see Eq. (4)) takes into account that the adsorption equilibrium has an influence on the adsorption rate and expresses that the rate – and thus, formally D_{app} – decreases with increasing strength of adsorption or more precisely with an increasing gradient of the loading with the concentration (here of naphthalene). For illustration, Fig. 2 displays the value of the particle porosity ε_p as well as of the factor K_p as a function of the concentration of naphthalene for the example of charcoal with a conversion of 60%. Both parameters are in the same order of magnitude for high concentrations. On the contrary, K_p is much larger than ε_p for lower concentrations, and D_{app} is then just given by the ratio D_{eff}/K_p . In this case, the amount of naphthalene diffusing into the particle is dominated by adsorption.

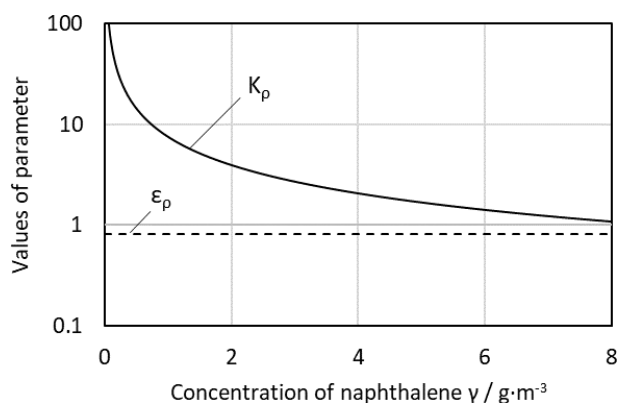


Figure 2. Influence of naphthalene concentration on particle porosity ε_p and factor K_p (70 °C, charcoal with $X = 0.59$).

As the porosity and tortuosity of the char particles have to be considered for the diffusion, the effective diffusion coefficient is used [12]:

$$D_{eff} = \frac{\varepsilon_p}{\tau} D_{12} \quad (6)$$

The binary diffusion coefficient D_{12} is taken from the equation given by Fuller et al. [13]:

$$D_{12} = \frac{1 \times 10^{-3} T^{1.75} \left(\frac{1}{M_1} + \frac{1}{M_2} \right)^{0.5}}{p \left[(\sum \Delta_1)^{0.33} + (\sum \Delta_2)^{0.33} \right]^2} \quad (7)$$

Knudsen diffusion is neglected since the main diffusion paths are meso-/macroporous.

4 Results and Discussion

4.1 Brunauer-Emmett-Teller Analysis

To characterize the charcoal samples, Brunauer-Emmett-Teller (BET) analysis was performed. The BET surface area of the raw charcoal from pyrolysis was determined to $61 \text{ m}^2 \text{ g}^{-1}$. A strong increase of the surface area to $453 \text{ m}^2 \text{ g}^{-1}$ is reached for 20% of char conversion by gasification with CO_2 . Thereafter, a slower and almost linear rise up to $884 \text{ m}^2 \text{ g}^{-1}$ at a conversion of 0.6 was measured (Tab. 2).

4.2 Adsorption Isotherms

To determine adsorption isotherms of naphthalene for the different charcoal samples, an adsorption temperature of 70 °C was chosen. This value was set as it is the target temperature for the gas at the outlet of the cooled adsorption section. Lower temperatures could fall below the dew point of the product gas and lead to condensation of water in the transfer line to the cogeneration unit. Experiments were performed with naphthalene concentrations in the range of $0.075\text{--}8 \text{ g m}^{-3}$ for the charcoal samples with a degree of conversion by CO_2 between 0.2

1) List of symbols at the end of the paper.

Table 2. BET results for charcoal samples produced by pyrolysis of wood pellets and subsequent gasification with CO₂ to a certain degree of conversion.

Degree of conversion (X) with CO ₂	Parameter	Value
0	S_{BET} [m ² g ⁻¹]	61
	$S_{\text{micropore}}$ [m ² g ⁻¹]	47
	$d_{\text{pore,av}}$ [nm]	2.4
0.23	S_{BET} [m ² g ⁻¹]	453
	$S_{\text{micropore}}$ [m ² g ⁻¹]	378
	$d_{\text{pore,av}}$ [nm]	2.4
0.33	S_{BET} [m ² g ⁻¹]	667
	$S_{\text{micropore}}$ [m ² g ⁻¹]	524
	$d_{\text{pore,av}}$ [nm]	2.4
0.59	S_{BET} [m ² g ⁻¹]	844
	$S_{\text{micropore}}$ [m ² g ⁻¹]	645
	$d_{\text{pore,av}}$ [nm]	2.6

and 0.6. The measured adsorption capacities, here denoted as the equilibrium load L_{eq} of the particles with naphthalene (in g per g charcoal), could best be described by a Freundlich isotherm [14] with γ_{naph} as naphthalene concentration (in g m⁻³) and K_{F} as the coefficient of the Freundlich isotherm:

$$L_{\text{eq}} = K_{\text{F}} \gamma_{\text{naph}}^{1/n} \quad (8)$$

All measured loads and the fitted Freundlich isotherms are presented in Fig. 3. The concentration range between 0 and 1 g m⁻³ is shown separately, as such low tar concentrations are needed for a fuel gas utilized in a technical cogeneration unit.

With regard to the concept of biomass gasification with integrated tar adsorption [1], a required equilibrium load of 0.3 g

tar per gram charcoal has been estimated for a charcoal conversion by gasification of 60 % and a tar content in the raw gas of 15 g g⁻¹ (see [1]). As a value of 0.38 g g⁻¹ is measured for the load, at least for the model substance naphthalene (Fig. 3), this goal can now be considered as attained.

The overall height of the isotherms shows a strong dependency on the measured BET surface area as described in Sect. 4.1. As the cooling section of the designed gasification plant is not isothermal, the relation between the temperature and the adsorption properties must be considered. In theory, the capacity of an adsorbent is a function of the adsorption potential A [15]:

$$A = RT \ln \left(\frac{c_{\text{sat}}}{c} \right) \quad (9)$$

c_{sat} denotes the saturation concentration of the adsorbate. From this equation, a temperature-dependent equation with ω_0 and E as fitting parameters was derived by Astakhov and Dubinin [16], which is used here to determine the temperature- and concentration-dependent equilibrium load:

$$L_{\text{eq}}(A) = \omega_0 e^{\left(\frac{-A}{E} \right)} \quad (10)$$

The pre-exponential parameter ω_0 depends on the (measured) BET surface area and, thus, on the charcoal conversion X (by CO₂). To obtain an adsorption capacity that includes the influence of the charcoal conversion X (by CO₂), the equation given by Dutta et al. [17] was applied:

$$\omega_0 = \omega_0(X=0) \left(1 + 100X^{\nu\beta} e^{-\beta X} \right) \quad (11)$$

The value of $\omega_0(X=0)$ was determined based on an adsorption experiment at 70 °C with a charcoal sample just prepared by pyrolysis of the wood pellets without subsequent treatment by CO₂ ($X=0$) and a naphthalene concentration of 5 g m⁻³.

To validate the temperature-dependent approach, two more experiments were performed at 100 °C and 120 °C, 5 g m⁻³ naphthalene concentration, and a conversion of 0.59. Fig. 4

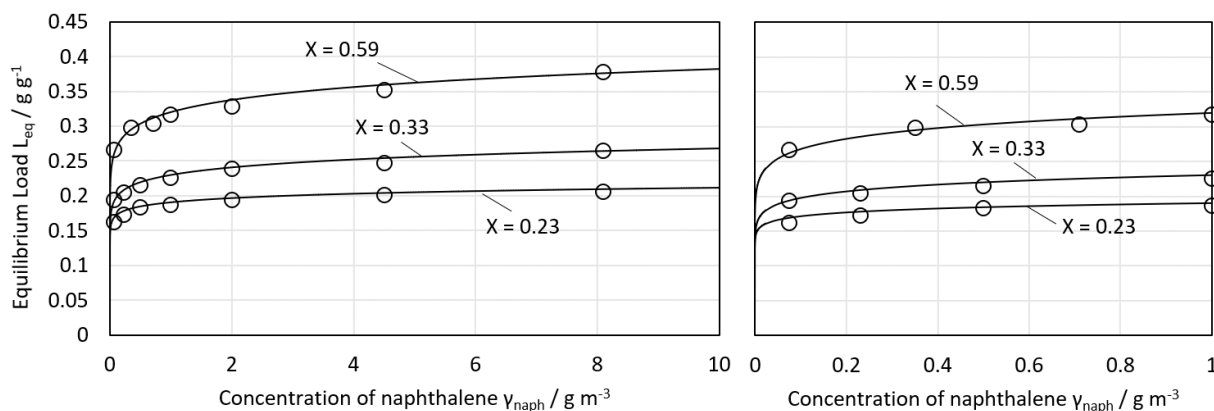


Figure 3. Freundlich isotherms for naphthalene on charcoal samples at different degrees of conversion by CO₂ during the preparation of the charcoal at 70 °C adsorption temperature (5 g sample weight, 0.075–8 g m⁻³ concentration of naphthalene, 200 L h⁻¹ N₂ (NTP) gas flow).

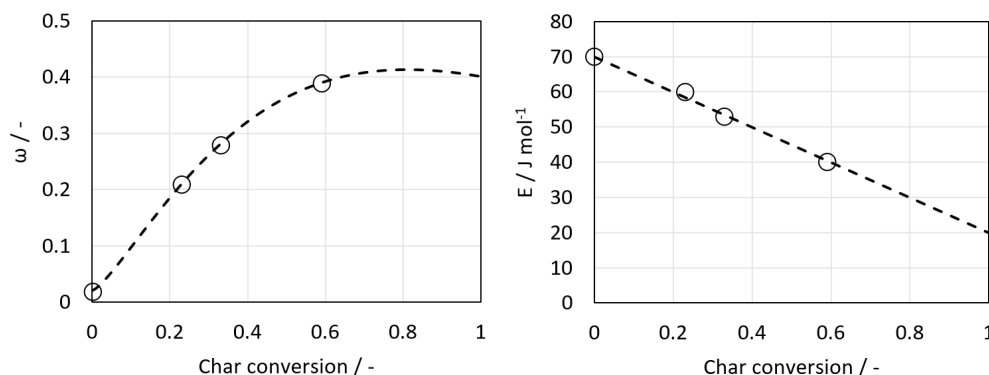


Figure 4. Model fit for parameters ω_0 and E of the Astakhov & Dubinin equation as a function of the char conversion by CO_2 during the preparation of the char coal (Eq. (11)).

illustrates the model fits of the parameters ω_0 and E . All experimental results and the universal model fits with Eq. (9) are indicated in Fig. 5. The fitting parameters for Eqs. (8) and (11) are given in Tab. 3.

Table 3. Parameters for Freundlich isotherms and Eq. (11).

Freundlich isotherms (Eq. (8))		
$X = 0.23$	$K_F [(\text{m}^3 \text{g}^{-1})^{1/22}]$	0.19
	$n [-]$	22
$X = 0.33$	$K_F [(\text{m}^3 \text{g}^{-1})^{1/15}]$	0.23
	$n [-]$	15
$X = 0.59$	$K_F [(\text{m}^3 \text{g}^{-1})^{1/13}]$	0.32
	$n [-]$	13
Eq. (11)		
$\omega_0 (X = 0) [-]$		0.02
$\beta [-]$		1.65
$\nu [-]$		0.81

4.3 Breakthrough Curves

In all experiments for different concentrations, the breakthrough curves have been logged to gain information about the

adsorption kinetics. For the implementation in the breakthrough model, the derivative of Eq. (9) with respect to the mass concentration has to be given for Eq. (5):

$$\frac{dL_{\text{eq}}}{d\gamma_n} = \frac{\omega_0 RT \left(\frac{M_n c_{\text{sat}}}{\gamma_n} \right)^{-\left(\frac{RT}{E} \right)}}{E \gamma_n} \quad (12)$$

For the unknown tortuosity τ (see Eq. (6)) the best model results were obtained assuming a linear decrease with increasing charcoal conversion X for conversions between 0 and 0.6:

$$\tau = 17.44 - 19.4X \quad (13)$$

More and larger diffusion paths are formed with increasing conversion of the charcoal by CO_2 during the sample preparation. Hence, τ is 17.4 for $X = 0$ and only 6 for $X = 0.59$.

The experimental and model results for the adsorption breakthrough curves at charcoal conversions of $X = 0.23, 0.33,$ and 0.59 are displayed in Fig. 6 for the three charcoal examples and initial naphthalene concentrations in a range of $0.5\text{--}5 \text{ g m}^{-3}$; the related values for the tortuosity of the charcoals are given in the captions.

The most accurate results are achieved for the samples with 59% char conversion. Predictions for the adsorption kinetics, as well as the integral of adsorbed mass are precise for all naphthalene concentrations. For the test series with a char conversion of 0.33, the kinetic behavior is predicted accurately.

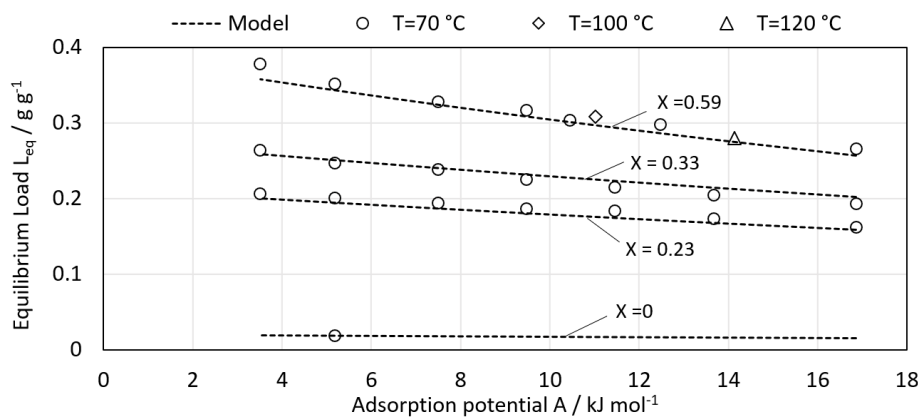


Figure 5. Experimental data and model results for equilibrium adsorption load of wood charcoal as a function of the adsorption potential (Eq. (9)), model fit with dependency of conversion (Eq. (10)), 5 g sample weight, $0.075\text{--}8 \text{ g m}^{-3}$ concentration of naphthalene, $200 \text{ L h}^{-1} \text{ N}_2$ (NTP) gas flow.

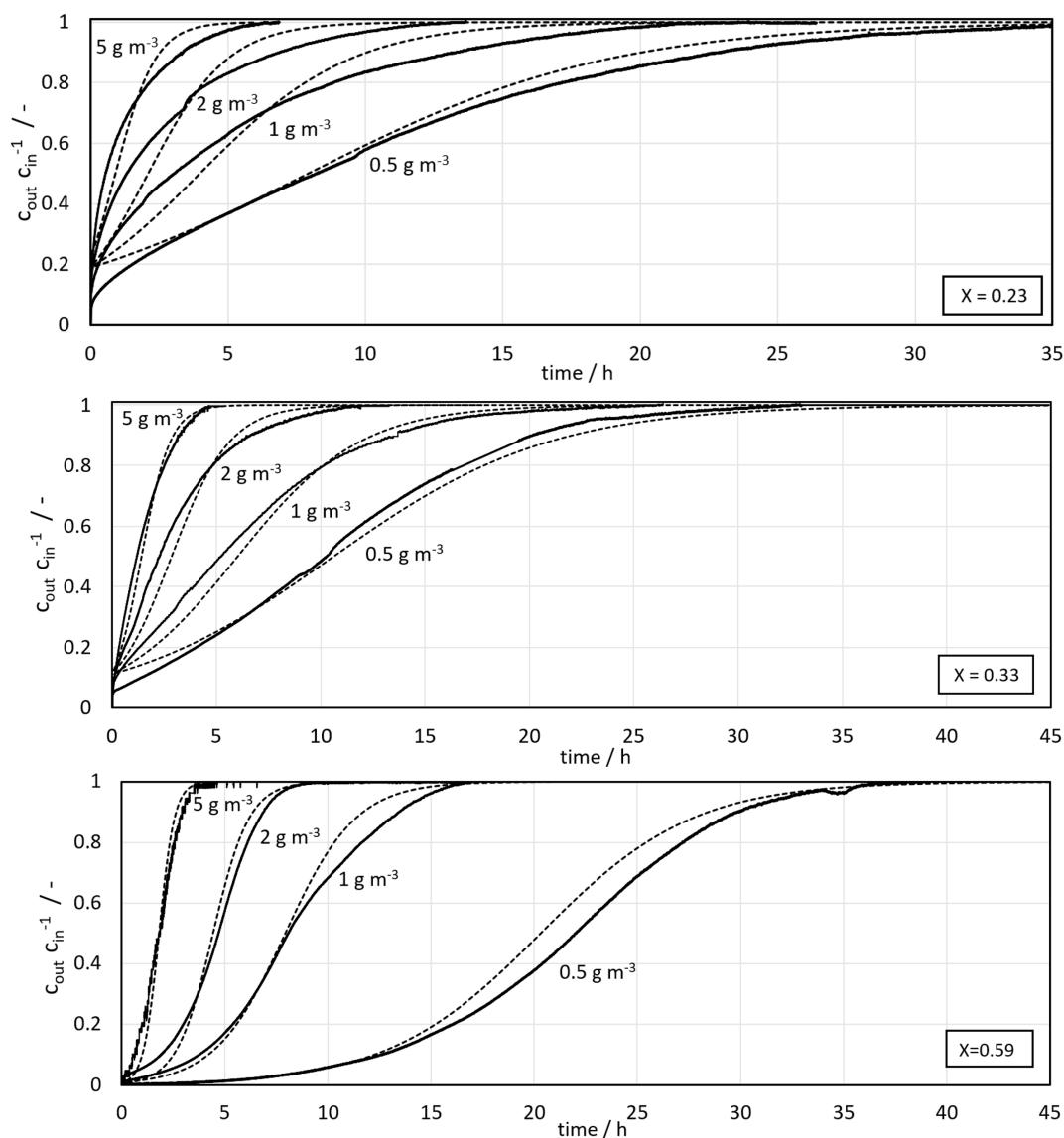


Figure 6. Breakthrough curves for naphthalene on charcoal samples with a char conversion of 0.23 (a), 0.33 (b), and 0.59 (c) at 70°C adsorption temperature, 5g sample weight, 0.5–5 g m⁻³ concentration of naphthalene, 200 L h⁻¹ N₂ (NTP) gas flow. Tortuosity τ is 13, 11, and 6 for $X = 0.23$, 0.33, and 0.59, respectively.

Nevertheless, a failure in the integral of adsorbed mass occurs as a result of the tolerances of the ω_0 parameter fit with Eq. (11). The predicted adsorption capacity therefore differs to a lower value in the model, as clearly visible in Fig. 6b. For samples with a char conversion of 23%, the adsorption kinetics of the model are slightly faster than the experimental results at higher concentrations but increasingly accurate at low naphthalene contents. The physical root of the slower diffusion rates should be determined in further experiments on the structure of the material. The mass integrals of these samples meet the experimental results.

For the charcoal samples with $X = 0.23$ and 0.33, a breakthrough was measured almost immediately due to the very short adsorption bed length of only 35 mm (Fig. 6). Only for $X = 0.59$ and rather low concentrations of naphthalene

(Fig. 6c), the breakthrough occurred after about 4 h. The mass of the samples was kept constant, but the bulk density of the bed decreased, and thus, the bed length increased significantly with rising char conversion. The aim of this study was not the determination of the breakthrough time, but the development of a reliable adsorption model. In case of a longer adsorption bed, the duration of the experiments would have prolonged excessively. Hence, this was not adjusted.

The model results for a much longer adsorption bed with 200 mm length as compared to the rather short bed length of the experiments with only 35 mm are illustrated in Fig. 7a for charcoals with a conversion degree X (during the preparation by CO₂) of 23%, 33%, and 59% conversion. For the inlet concentration of naphthalene, a value of 0.5 g m⁻³ was assumed. Now, the breakthrough would occur after about 20 h, which is

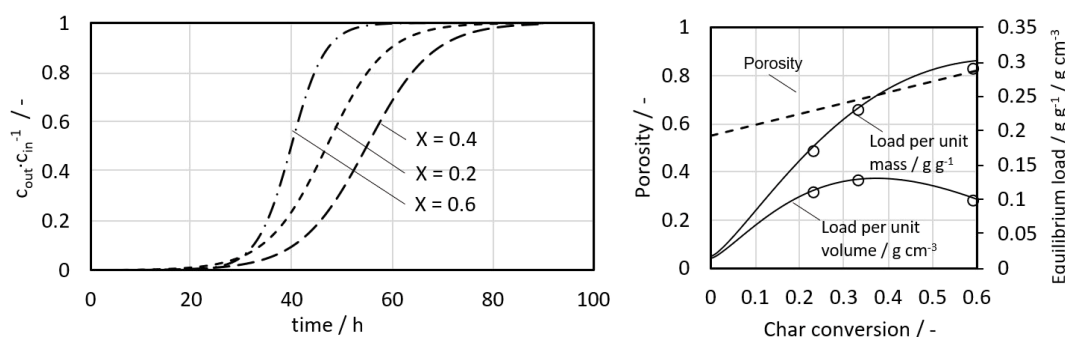


Figure 7. (a) Calculated breakthrough curves for naphthalene in a 200-mm charcoal adsorption bed with a charcoal conversion (during the preparation/treatment with CO₂) of 0.2, 0.4, and 0.6 (70 °C adsorption temperature, 0.5 g m⁻³ inlet concentration of naphthalene, 200 L h⁻¹ N₂ (NTP) gas flow). (b) Influence of degree of charcoal conversion on the particle porosity and on the equilibrium adsorption load per mass and per volume of the particles.

a value acceptable for technical applications. For this bed length, the charcoal with $X = 0.59$ (and the highest internal surface area, see Tab. 2) provides the steepest breakthrough curve but the lowest volumetric adsorption capacity. The latter fact is due to an increment of the particle porosity with increasing value of X (0.66 for $X = 0.23$ and 0.82 for $X = 0.59$, Tab. 1) and, therefore, a reduction of the charcoal mass for a given bed length (here 200 mm). The highest volumetric load with naphthalene is reached for a charcoal of about 33 % conversion (Fig. 7b).

Note that in the concept of a concurrent gasification with integrated subsequent adsorption, as outlined in Sect. 1 and in [1, 2], the adsorption would be, strictly speaking, not conducted in a fixed-bed but in a moving-bed adsorber. In this case, the amount of charcoal leaving the gasification section has to be sufficiently high to avoid a breakthrough at any time, i.e., the velocity of the adsorption front has to be lower than the velocity of migration of the charcoal by gravity, but the discussion of these aspects is beyond the scope of this work.

5 Summary and Outlook

Experimental data of the adsorption of naphthalene on different charcoals in terms of adsorption isotherms and breakthrough curves are presented. The charcoals were produced from wood pellets by pyrolysis and subsequent partial gasification with CO₂ until a certain conversion (X) of the raw charcoal (after pyrolysis) of up to 59 % was reached. Naphthalene was used as a model substance for various tar species present in the product gas of biomass gasification.

A transient one-dimensional adsorption model was developed to predict the breakthrough curve for different values of conversion X , initial naphthalene concentration, and adsorption temperature. This kinetic adsorption model considers the temperature- and concentration-dependent equilibrium load, here described by a Freundlich isotherm, as well as the influence of conversion X on the change of structural parameters such as the tortuosity and, thus, on the effective diffusion in the porous charcoal particles. The model agrees well with the experimental results and can now be applied for the design of

the cooled adsorption section in a plant for biomass gasification with integrated tar adsorption.

The authors have declared no conflict of interest.

Acknowledgement

Open access funding enabled and organized by Projekt DEAL.

Symbols used

A	[J mol ⁻¹]	adsorption potential
c	[mol m ⁻³]	concentration
d	[m]	diameter
D	[m ² s ⁻¹]	diffusion coefficient
E	[J mol ⁻¹]	fitting parameter equilibrium load equation
K_F	[(m ³ kg ⁻¹) ^{1/n}]	Freundlich isotherm coefficient
k_{LDF}	[s ⁻¹]	linear driving force factor
K_p	[-]	inhibiting factor
L	[g g ⁻¹]	adsorption load
M	[kg mol ⁻¹]	molar mass
n	[-]	Freundlich isotherm coefficient
p	[Pa]	pressure
R	[J kg ⁻¹ mol ⁻¹]	gas constant
t	[s]	time
T	[K]	absolute temperature
u	[m s ⁻¹]	velocity
X	[-]	conversion

Greek letters

β	[-]	fitting parameter for inner surface equation
γ	[kg m ⁻³]	mass concentration
Δ	[-]	diffusion volume
ε	[-]	porosity

ν	[-]	fitting parameter for inner surface equation
ρ	[kg m ⁻³]	density
τ	[-]	tortuosity
ω_0	[-]	fitting parameter equilibrium load equation

Sub- and superscripts

12	binary
Ad	adsorption
ads	adsorbed
app	apparent
av	average
b	bulk
BET	Brunauer-Emmett-Teller
c	charcoal
cur	current
eff	effective
eq	equilibrium
LDF	linear driving force
n	naphthalene
p	particle
s	superficial
sat	saturation

Abbreviations

BET	Brunauer-Emmett-Teller
NTP	normal temperature and pressure

References

- [1] A. Gradel, R. Honke, J. A. Wüning, T. Plessing, A. Jess, *Chem. Eng. Technol.* **2019**, *42* (9), 1895–1906. DOI: <https://doi.org/10.1002/ceat.201800640>
- [2] J. A. Wüning, *European Patent EP000003088492B1*, **2015**.
- [3] W. Kast, *Adsorption aus der Gasphase*, VCH, Weinheim **1988**.
- [4] M. Danish, T. Ahmad, *Renewable Sustainable Energy Rev.* **2019**, *42* (9), 1895–1906. DOI: <https://doi.org/10.1016/j.surfin.2018.02.001>
- [5] Y. Liu, Z. Li, Y. Xiong, Y. Xing, C. Tsai, Q. Yang, Z. Wang, R. T. Yang, *RSC. Adv.* **2016**, *6*, 21193–21203. DOI: <https://doi.org/10.1039/c5ra27289k>
- [6] A. M. Mastral, T. Garcia, M. S. Callen, M. V. Navarro, J. Galban, *Environ. Sci. Technol.* **2001**, *35*, 2395–2400. DOI: <https://doi.org/10.1021/es000152u>
- [7] Y. Shen, Y. Zhou, Y. Fu, N. Zhang, *Renewable Energy* **2020**, *146*, 1700–1709. DOI: <https://doi.org/10.1016/j.renene.2019.07.167>
- [8] X. Zhang, J. Pan, L. Wang, H. Sun, Y. Zhu, H. Chen, *Chin. J. Chem. Eng.* **2019**, *28* (1), 279–285. DOI: <https://doi.org/10.1016/j.cjche.2019.06.007>
- [9] DIN EN 14961-2, *Solid Biofuels – Fuel Specifications and Classes – Part 2: Wood Pellets for Non-industrial Use*, Beuth, Berlin **2011**.
- [10] A. Gradel, *Vergasung biogener Reststoffe mit integrierter Adsorption von Teerbestandteilen*, Ph.D. Thesis, University Bayreuth **2021**.
- [11] E. Glückauf, *J. Chem. Soc. Faraday Trans.* **1955**, *51*, 1540–1551. DOI: <https://doi.org/10.1039/TF9555101540>
- [12] *Chemical Technology* (Eds: A. Jess, P. Wasserscheid), Wiley-VCH, Weinheim **2013**.
- [13] E. N. Fuller, P. D. Shettler, J. Giddings, *Ind. Eng. Chem.* **1966**, *58* (5), 18–27. DOI: <https://doi.org/10.1021/ie50677a007>
- [14] H. Freundlich, *Z. Phys. Chem.* **1907**, *57*, 385–470. DOI: <https://doi.org/10.1515/zpch-1907-5723>
- [15] M. Polanyi, *Science* **1963**, *141*, 1010–1013. DOI: <https://doi.org/10.1126/science.141.3585.1010>
- [16] V. A. Astakhov, M. M. Dubinin, *Russ. Chem. Bull.* **1971**, *20* (1), 3–7. DOI: <https://doi.org/10.1007/bf00849307>
- [17] S. Dutta, C. Y. Wen, R. J. Belt, *Ind. Eng. Chem. Process Des. Dev.* **1977**, *16* (1), 20–30. DOI: <https://doi.org/10.1021/i260061a004>